Revelation of Preferences in Trip Distribution Models

Kurt Jörnsten⁽¹⁾, Inge Thorsen⁽²⁾, and Jan Ubøe⁽¹⁾

⁽¹⁾Norwegian School of Economics and Business Administration, Helleveien 30, N-5045 Bergen, Norway.

⁽²⁾Stord/Haugesund College, Bjørnsonsgate 45, 5528 Haugesund, Norway.

ABSTRACT. In this paper we will see how commuter preferences can be revealed from observations of trip distributions. We will explain how to find unique representations of preference structures leading to an observed trip distribution, and will also present a numerical method that can be used to infer preferences from systems of considerable size. The theory is applied to a real world network, and we show how our framework can be used to reveal detailed information about the spatial structure of this network. We also use this new framework to suggest a new approach to evaluate the impact of road pricing.

Keywords: Travel demand, revealed preferences, efficient distance, road pricing Jel codes: C31, R41, R48

1. Introduction

We consider a network of N towns, and we let T_{ij} denote the number of commuters from i to j, i, j = 1, ..., N. Our aim is to study trip distributions in this system, and to this end we make use of a doubly constrained gravity model on the form

$$T_{ij} = A_i B_j \exp[U_{ij}]$$

$$\sum_{i=1}^{N} T_{ij} = E_j \text{ for } j = 1, \dots, N \qquad \sum_{i=1}^{N} T_{ij} = L_i \text{ for } i = 1, \dots, N \qquad (1)$$

where $\mathbf{E} = (E_1, E_1, \dots, E_N)$ and $\mathbf{L} = (L_1, L_2, \dots, L_N)$ are given vectors, and U_{ij} measures the (dis)utility of commuting between town *i* and *j*, *i*, *j* = 1, ..., *N*. A model of this type is well founded within the theory of regional science. The simplest derivation of this kind of model is based on the cost efficiency principle, see Erlander and Smith (1990). The basic idea is that states with high total utility should be more probable than states with low total utility. If this principle holds in general, it is possible to prove that the system settles at a statistical equilibrium given by (1), see, e.g., Erlander and Smith (1990), Jörnsten and Ubøe (2005).

The most commonly used version of this problem is probably the case with $U_{ij} = -\beta d_{ij}$, where β is a constant and d_{ij} denotes the geographical distance between the towns. A model of this kind is often referred to as the standard gravity model. Wilson (1967) showed that the standard gravity model can be derived from entropy maximizing principles. Several other lines of approach leads to the same model, however. Anas (1983) was the first to show that the standard gravity model can be derived from random utility theory, and we refer to Erlander and Stewart (1990) for a number of different derivation of this model. The number of applications are too many to be covered here, we refer insted to the seminal textbook of Sen and Smith (1995), and the references therein.

The basic problem we want to study in this paper can be described as follows:

Given an observed trip distribution $\mathbf{T}^{\text{observed}} = \{T_{ij}\}_{i,j=1}^{N}$ find a utility matrix $\mathbf{U} = \{U_{ij}\}_{i,j=1}^{N}$ such that the matrix \mathbf{T} given by (1) replicates $\mathbf{T}^{\text{observed}}$.

There is a number of good reasons, however, why one should normally *not* attempt to solve a problem of this kind. The first major objection is that the problem is ill posed. If there exists a solution, it is easy to see that there must exist numerous other solutions to the problem. Hence unique solutions cannot be found. Second, in all but exceptional cases it is more or less impossible to solve non-linear problems with more than say 20-30 parameters. Unless N is so small that the problem is only of academic interest ($N \le 5$), we quickly face problems with several hundred parameters; a setting that is normally out of reach for numerical computation.

With the above remarks in mind it is hence quite surprising that problems of the above type can be solved. Not only can they be solved, unique solutions can be obtained in a strictly rigorous sense, and systems of considerable size (N > 15) can be solved quickly by what appears to be a very robust numerical method. The paper is organized as follows: In Section 2 we consider questions related to uniqueness, and show that each trip distribution pattern can be represented by a unique utility matrix with zeros in the first row and in the first column. In Section 3 we present the numerical algorithm, and report some results based on a series of computer experiments. In Section 4 we consider alternative representations of utility matrices. The particular representation used in Sections 2 and 3 is very simple to implement in a computer program. Results are hard to interpret, however. That calls for alternative, more transparent representations. We discuss several different representations through a small size (5 node) network, and in particular we develop the notion of *efficient distances*. In Section 5, we consider a larger (13 nodes) real world network using real world data. We use the construction of efficient distances developed in Section 4 to analyze the observed trip distribution, and show how this reveals lots of detailed information about the spatial structure of the system. In Section 6 we suggest an application of this modeling framework to road pricing. Finally in Section 7 we offer some concluding remarks.

2. Canonical representation of utilities

To find a numerical solution to (1), we need to construct a set of balancing factors

$$A_1,\ldots,A_N,B_1,\ldots,B_N$$

This is easily done using the classical Bregman balancing algorithm, see Bregman (1967). Without loss of generality we can assume that $A_1 = 1$, and then there exist a unique set of balancing factors $A_1, \ldots, A_N, B_1, \ldots, B_N$ providing a solution to (1). Many different utility matrices U may lead to the same trip distribution matrix T, however. Technically speaking, this partitions the space of utility matrices into equivalence classes, and the way to obtain uniqueness is then to single out a unique representative from each equivalence class. A special kind of representation is obtained via the following simple transformation

$$\tilde{U}_{ij} = U_{ij} - U_{i1} - U_{1j} + U_{11} \qquad i, j = 1, \dots, N$$
(2)

LEMMA 2.1

Let $\mathbf{U} = \{U_{st}\}_{s,t=1}^{M,N}$ be given, let $\tilde{\mathbf{U}}$ be defined by (2) and let \mathbf{T} and $\tilde{\mathbf{T}}$ denote the corresponding flows from (1) when we use \mathbf{U} and $\tilde{\mathbf{U}}$, respectively. Then $\mathbf{T} = \tilde{\mathbf{T}}$.

PROOF

Let $A_1, \ldots, A_N, B_1, \ldots, B_N$ denote the balancing factors solving (1) when we use U, and define

$$\tilde{A}_{i} = A_{i} \exp[U_{i1} - U_{11}] \quad i = 1, \dots, N
\tilde{B}_{j} = B_{j} \exp[U_{1j}] \quad j = 1, \dots, N$$
(3)

Then

$$\tilde{A}_{i}\tilde{B}_{j}\exp[\tilde{U}_{ij}] = A_{i}\exp[U_{i1} - U_{11}]B_{j}\exp[U_{1j}]\exp[U_{ij} - U_{i1} - U_{1j} + U_{11}]$$

$$= A_{i}B_{j}\exp[U_{ij}]$$
(4)

Note that $\tilde{A}_1 = A_1 = 1$. Hence $\tilde{A}_1, \ldots, \tilde{A}_T, \tilde{B}_1, \ldots, \tilde{B}_S$ are the unique balancing factors providing a solution to (1). (4) then shows that $\mathbf{T} = \tilde{\mathbf{T}}$.

Lemma 2.1 says that the resulting trip distribution does not change when we change U to \tilde{U} . This is a quite trivial observation, and not important in its own right. The important issue, however, is that the transformation $U \mapsto \tilde{U}$ singles out a unique representative from each equivalence class. The following proposition clarifies this.

PROPOSITION 2.2

Let $\mathbf{U}^{(1)}$ and $\mathbf{U}^{(2)}$ denote two utility matrices, and assume that $\mathbf{T}^{(1)} = \mathbf{T}^{(2)}$. Then $\tilde{\mathbf{U}}^{(1)} = \tilde{\mathbf{U}}^{(2)}$.

PROOF

It follows from Lemma 1.1 that $\tilde{\mathbf{T}}^{(1)} = \tilde{\mathbf{T}}^{(2)}$. Hence from (1) we know that

$$\tilde{A}_{i}^{(1)}\tilde{B}_{j}^{(1)}\exp[\tilde{U}_{ij}^{(1)}] = \tilde{A}_{i}^{(2)}\tilde{B}_{j}^{(2)}\exp[\tilde{U}_{ij}^{(2)}]$$
(5)

Put i = 1, and observe that $\tilde{U}_{s1}^{(1)} = \tilde{U}_{s1}^{(2)} = 0$ by construction. Since $\tilde{A}_{1}^{(1)} = \tilde{A}_{1}^{(2)} = 1$, it follows that $\tilde{B}_{j}^{(1)} = \tilde{B}_{j}^{(2)}$ for all j = 1, ..., N. In particular we get $\tilde{B}_{1}^{(1)} = \tilde{B}_{1}^{(2)}$. Put j = 1 in (5) and observe that $\tilde{U}_{j1}^{(1)} = \tilde{U}_{j1}^{(2)} = 0$. It then follows from (5) that $\tilde{A}_{i}^{(1)} = \tilde{A}_{i}^{(2)}$ for all i = 1, ..., N. Hence all the balancing factors are equal, and it follows from (5) that we must have $\tilde{U}_{ij}^{(1)} = \tilde{U}_{ij}^{(2)}$ for all i and j.

Note that the transformation defined by (2) forces zeros in the first row and the first column. The following corollary is hence a direct consequence of Proposition 2.2.

COROLLARY 2.3

Assume that an observed flow \mathbf{T} can be replicated by a model that satisfies (1). Then we can find a unique utility matrix \mathbf{U} on the form

$$\mathbf{U} = \begin{bmatrix} 0 & 0 & 0 & \dots & 0 \\ 0 & a_{11} & a_{12} & \dots & a_{1(N-1)} \\ 0 & a_{21} & a_{22} & \dots & a_{2(N-1)} \\ \vdots & \vdots & \vdots & \vdots & \vdots \\ 0 & a_{(N-1)1} & a_{(N-1)2} & \dots & a_{(N-1)(N-1)} \end{bmatrix}$$
(6)

that replicates **T**.

3. The numerical algorithm

Corollary 2.3 greatly facilitates numerical calibrations. It is sufficient to search for solutions of the form (6), and the replicating utilities of this form are unique. Unless N is very small, however, we are still faced with a model with a vast number of parameters, and standard replication software cannot possibly handle a system of that sort. A very naive, yet surprisingly efficient idea comes to our rescue:

Choose and fix any pair (i, j). When we change U_{ij} we primarily change the corresponding entry T_{ij} in \mathbf{T} , and the effect on the other entries is smaller.

To replicate an observed matrix $T^{\rm observed}$, we hence exploit the following algorithm:

1. Initially, put all $U_{ij} = 0, i, j = 1, ..., N$.

2. Fix all entries in U except U_{22} , and find a value on U_{22} such that $\mathbf{T}_{22} = \mathbf{T}_{22}^{\text{observed}}$. Update U_{22} to this particular value.

3. Fix all entries in U except U_{23} , and find a value on U_{23} such that $\mathbf{T}_{23} = \mathbf{T}_{23}^{\text{observed}}$. Update U_{23} to this particular value.

4. We continue like that until we have updated all entries of U with i, j = 2, ..., N.

5. The procedure 2-4 above is repeated until the system settles at a replicating state.

In the procedure above, each step involves only one variable at the time, and due to the extreme speed of the Bregman balancing, the updates can be constructed in milliseconds. We have tried out this procedure on a number of different test cases, and the results were quite surprising. The simulations were all carried out on a fairly slow computer, and we never invested much effort to optimize the code. Nevertheless, we were able to solve systems as big as 15×15 (a problem with no less than 196 variables!) in less than 24 hours. This certainly means that much larger systems can be handled. The method also appears to be very robust. In numerical methods of this sort, it is often critical that one starts out with a very good initial value. In all cases we have tried so far, we only used the origin as our initial guess. Still we have never encountered cases where this algorithm failed to find the correct solution.

We should remark, however, that far from all networks are suitable for an analysis of the above kind. Clearly the system degenerates in situations with zero-entries. Hence such cases cannot be covered, at least not directly. In cases where the observed trip distribution contains a few very large and a few very small (but non-zero) elements, the algorithm can still be used but uses much more time to settle.

In the real world example we discuss in Section 5, we encountered several numerical problems. The observed trip distribution contained a few very small entries, with one entry equal to zero. This could certainly been avoided if we had used a less refined partition, but we wanted to test the limitations of the framework. As a first step we put the zero entry equal to 1. The system then used several days to settle, but a solution could still be found. To test the robustness of the system, we perturbed several of the smallest entries. As a result of this, we could observe a significant change in the utilities attached to the perturbed entries, while the rest of the system appeared to be quite robust.

From our experiments we recommend that this framework is used to study networks with a moderate spatial separation and where zones are sufficiently large to avoid very small entries, zero entries in particular. The ideal application is probably a major city separated into 5-20 reasonably large zones. In our test cases we mostly considered cases where the size of the entries differ by no more than 2 orders of magnitude. The algorithm is then very fast. More extreme cases can certainly be covered, but at a cost of computation speed.

4. Alternative representations and efficient distances

Consider the network in Figure 1 below, where we assume that $d_{12} = d_{23} = d_{45} = 20$ (km), and $d_{24} = 60$ (km).

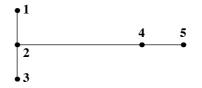


FIGURE 1: A 5-node system

The number of workers and employment opportunities are defined as follows:

$$L_1 = 1000, L_2 = 1000, L_3 = 1000, L_4 = 5000, L_5 = 2000$$

$$E_1 = 1500, E_2 = 2500, E_3 = 1500, E_4 = 3000, E_5 = 1500$$
(7)

As mentioned in the introduction, a standard approach to trip distributions is to assume that the (dis)utility of commuting is proportional to the distance between the the alternatives, i.e., that

$$U_{ij} = -\beta \, d_{ij} \tag{8}$$

If we assume that $\beta = 0.01$, we end up with a utility matrix

$$\mathbf{U} = \begin{bmatrix} 0 & -0.2 & -0.4 & -0.8 & -1. \\ -0.2 & 0 & -0.2 & -0.6 & -0.8 \\ -0.4 & -0.2 & 0 & -0.8 & -1. \\ -0.8 & -0.6 & -0.8 & 0 & -0.2 \\ -1. & -0.8 & -1. & -0.2 & 0 \end{bmatrix}$$
(9)

This utility matrix can be inserted in (1) together with (7), and we can then solve (1) to get the following trip distribution

$$\mathbf{T} = \begin{bmatrix} 269 & 319 & 180 & 160 & 72\\ 198 & 350 & 198 & 175 & 79\\ 180 & 319 & 269 & 160 & 72\\ 623 & 1103 & 623 & 1829 & 823\\ 230 & 408 & 230 & 677 & 454 \end{bmatrix}$$
(10)

If we use (2) to convert the utilities to a representing form, we get

$$\tilde{\mathbf{U}} = \begin{bmatrix} 0 & 0. & 0. & 0. & 0. \\ 0. & 0.4 & 0.4 & 0.4 & 0.4 \\ 0. & 0.4 & 0.8 & 0.4 & 0.4 \\ 0. & 0.4 & 0.4 & 1.6 & 1.6 \\ 0. & 0.4 & 0.4 & 1.6 & 2. \end{bmatrix}$$
(11)

According to Lemma 2.1, the utility matrices given by (9) and (11) both give the trip distribution reported in (10). Moreover, the utility matrix given by (11) is the *only* utility matrix with zeros in the first row and first column that gives the trip distribution in (10). The downside with (11), however, is that it is not so easy to interpret, excluding of course the obvious fact that it is really equivalent to (9). To examine this further, we will consider a more realistic situation.

In a real world empirical analysis, one never observes that observations are in perfect accordance with a standard gravity model. The best one can hope is to find a replicant that is not too different in the sense that the replicant captures some main effects. To examine this further, let us assume that we have observed

$$\mathbf{T}^{\text{observed}} = \begin{bmatrix} 269 & 319 & 180 & 160 & 72\\ 198 & 350 & 198 & 175 & 79\\ 180 & 319 & 269 & 160 & 72\\ 623 & 1103 & 623 & 1779 & 873\\ 230 & 408 & 230 & 727 & 404 \end{bmatrix}$$
(12)

Note that the trip distributions in (10) and (12) are different; inspect the lower right corner. The standard approach to analyze (12) would be to find the best replication by a standard gravity model. The calculations are straightforward, and the best replication (in the sense of maximum loglikelihood) is obtained using $\hat{\beta} = 0.00974131$, in which case we get

$$\mathbf{T}^{\text{replication}} = \begin{bmatrix} 265 & 318 & 180 & 163 & 74 \\ 197 & 348 & 197 & 178 & 81 \\ 180 & 318 & 265 & 163 & 74 \\ 626 & 1106 & 626 & 1820 & 822 \\ 232 & 410 & 232 & 675 & 450 \end{bmatrix}$$
(13)

We observe that (12) and (13) are different, but this modeling framework offers no opportunity to explain *why* they are different. The model in (1) used together with Corollary 2.3 provides much more detailed information, however. Using the algorithm described in Section 3, we get perfect replication at

$$\tilde{\mathbf{U}} = \begin{bmatrix} 0 & 0 & 0 & 0 & 0 \\ 0 & 0.399 & 0.402 & 0.396 & 0.399 \\ 0 & 0.402 & 0.803 & 0.402 & 0.402 \\ 0 & 0.401 & 0.402 & 1.569 & 1.655 \\ 0 & 0.403 & 0.402 & 1.67 & 1.881 \end{bmatrix}$$
(14)

and this is the only utility matrix of this form that gives perfect replication. If we compare (11) with (14), we notice that there are substantial differences in the lower right corner, but apart from that the results are not very easy to interpret. Hence it might be profitable to look for more transparent representations. Many options are available, and we will discuss only a few.

Alternative representations

Although the matrix given by (14) provides a unique representation within the class of matrices on the form (6), there are many other ways of representation. Roughly speaking we will obtain a unique representation whenever we put 2n - 1 linear restrictions on the system. Instead of forcing zeros in the first row and first column, we might assume that the average must be zero in all rows and in all columns. The unique representative within this particular class is then given by

$$\mathbf{U} = \begin{bmatrix} 0.479 & 0.159 & 0.078 & -0.328 & -0.388\\ 0.16 & 0.239 & 0.16 & -0.251 & -0.308\\ 0.078 & 0.159 & 0.48 & -0.328 & -0.388\\ -0.326 & -0.246 & -0.326 & 0.436 & 0.462\\ -0.392 & -0.31 & -0.392 & 0.471 & 0.622 \end{bmatrix}$$
(15)

The results are still quite difficult to interpret. Most researchers in this field have been working with utilities given in the form from (8) and (9), however, and hence it might be profitable to convert the results to a similar form. There is no unique conversion of this form, but one option is to impose conditions where we have, e.g.

- a) Zeros on the diagonal
- b) Symmetry in the *i*th row versus the *i*th column

We let $U^{(i)}$ denote a representation of this special form. A representation with symmetry in the first row versus versus the first column, is given by

$$\mathbf{U}^{(1)} = \begin{bmatrix} 0 & -0.2 & -0.402 & -0.784 & -0.941 \\ -0.2 & 0 & -0.2 & -0.588 & -0.741 \\ -0.402 & -0.2 & 0 & -0.784 & -0.941 \\ -0.784 & -0.583 & -0.784 & 0 & -0.07 \\ -0.941 & -0.738 & -0.941 & -0.055 & 0 \end{bmatrix}$$
(16)

This approach admits an interpretation in terms of efficient distances. If we use the replication parameter $\hat{\beta} = 0.00974131$ and convert utilities to *efficient distances* via

$$d_{ij}^{(i)} = -\frac{U_{ij}^{(i)}}{\hat{\beta}}$$
(17)

we obtain an efficient distance matrix

$$\mathbf{d}^{(1)} = \begin{bmatrix} 0 & 20.5 & 41.3 & 80.7 & 96.8\\ 20.5 & 0 & 20.5 & 60.5 & 76.2\\ 41.3 & 20.5 & 0 & 80.7 & 96.8\\ 80.7 & 60. & 80.7 & 0 & 7.2\\ 96.8 & 75.9 & 96.8 & 5.6 & 0 \end{bmatrix}$$
(18)

A clear advantage with this approach is that it leaves matrices of the form given by (8) and (9) invariant. I.e., if we start out with a model where the utilities are defined by (8) and (9), the efficient distances defined by (17) are all equal to the original distance matrix.

When data does not admit perfect replication by a standard gravity model (which is always the case with real world data), the representations $\mathbf{U}^{(1)}, \mathbf{U}^{(2)}, \dots, \mathbf{U}^{(N)}$ will be slightly different, and the same applies to the efficient distances defined by (17). To reduce this bias, we suggest that one should use the average value of all these representations, i.e., use a representation

$$\overline{\mathbf{U}} = \frac{1}{N} \sum_{i=1}^{N} \mathbf{U}^{(i)} \tag{19}$$

Since all the components are unique, this representation is unique as well. Once this is done, we can define a new efficient distance matrix \overline{d} via

$$\overline{d}_{ij} = -\frac{\overline{U}_{ij}}{\hat{\beta}} \tag{20}$$

The representation defined by (19) and (20) is our preferred approach, and we will use that approach when we analyze the real world network in the next section.

In the example above, we get the final results

$$\overline{U} = \begin{bmatrix} 0 & -0.2 & -0.4 & -0.79 & -0.94 \\ -0.2 & 0 & -0.2 & -0.59 & -0.74 \\ -0.4 & -0.2 & 0 & -0.79 & -0.94 \\ -0.78 & -0.58 & -0.78 & 0 & -0.07 \\ -0.94 & -0.74 & -0.94 & -0.06 & 0 \end{bmatrix}$$
(21)
$$\overline{\mathbf{d}} = \begin{bmatrix} 0 & 20.6 & 41.3 & 80.8 & 96.6 \\ 20.4 & 0 & 20.4 & 60.5 & 76. \\ 41.3 & 20.6 & 0 & 80.8 & 96.6 \\ 80.6 & 60. & 80.6 & 0 & 6.9 \\ 97. & 76.2 & 97. & 5.9 & 0 \end{bmatrix}$$
(22)

We notice that the efficient distances in (18) and (22) are only slightly different.

If we compare these distances to the original distance matrix d

$$\mathbf{d} = \begin{bmatrix} 0 & 20 & 40 & 80 & 100\\ 20 & 0 & 20 & 60 & 80\\ 40 & 20 & 0 & 80 & 100\\ 80 & 60 & 80 & 0 & 20\\ 100 & 80 & 100 & 20 & 0 \end{bmatrix}$$
(23)

we notice in particular some distinct features in the lower right corner. The external commuting between these nodes is (by construction of the data) much larger than apriori expectations. One way of interpreting this is to say that the efficient distance between these nodes (from (22)) is much smaller than the geographical distance that we observe in (23).

$Some \ technical \ remarks$

To compute the various representations in (19) and (20), one needs to solve a moderate number of linear equations; see the Appendix for a detailed description of these equations. Such computations can be done very quickly, and regardless of the size of the system it takes less than 1 second even on a fairly slow computer. The timeconsuming part is to use the algorithm in Section 3 to compute the representation (6) in Corollary 2.3. Once this is done, it is almost instantly converted to the more transparent form defined by (19) and (20).

The value of the replication parameter $\hat{\beta}$ depends on what measure of fit we use. If we instead of maximum loglikelihood use minimum SRMSE, we get $\hat{\beta} = 0.00933947$. This would define yet another slightly different efficient distance matrix.

5. Application to a real world network

Our real world example is based on data from a region in the southern parts of Western Norway, see the map in Figure 2. The seven municipalities in the region have a total of about 96000 inhabitants. Haugesund is the regional center, with a population of about 32000 inhabitants. The region comes close to what is defined as "an economic area" in Barkley et al. (1995), with a relatively self-contained labor market. The high degree of intra-dependency is due to physical, topographical, transportation barriers, that lengthen travel distances, and thereby deter labor market interaction with other regions. This natural delimitation of the region contributes to make it appropriate for our purpose. The area is relatively sparsely populated, but the dominating part of the spatial labor market mobility is intraregional, even for the zones at the outer edges of the region. At the chosen level of zonal spatial aggregation, commuting flows are observed between practically all of the zones in the region.



Figure 2: The region and the transportation network

The nodes approximately represent the geographical center of gravity in their respective zones. Information on commuting flows and interzonal distances is originally collected at a more disaggregated spatial level, corresponding to a division of the region into 60 postal delivery zones. This is the most detailed level of information that is available on individual residential and work location. The information is provided for us as preliminary data by Statistics Norway, it refers to the 4th quarter of 2004, and is based on the Employer-Employee register. The matrices of physical distances and traveling times were prepared for us by the Norwegian Mapping Authorities. Information on speed limits and road categories is converted into traveling times through instructions worked out by the Institute of Transport Economics, and the center of each (postal delivery) zone is found through detailed information on residential densities and the road network. Both the distances and traveling times are constructed from a shortest route algorithm. The same set of principles is used in aggregating from the geography of 60 zones to the 13-node network description of the geography appropriate for our purpose in this paper.

The matrices (24) and (25), see the appendix, represent spatial separation between the zones in terms of physical distance (km) and traveling time (minutes), respectively. The differences between the two matrices reflect speed limits and road categories.

As mentioned above the natural delimitation of the region contributes to make it appropriate for our purpose. In other respects the region is not appropriate, however. Distances are rather long between zones at the outer edges of the region, and the region is relatively sparsely populated. This results in a commuting flow matrix with some rather small entries, see the commuting flow matrix (26). As stated above our algorithm is best suited for systems where entries do not differ by a very high order of magnitude. To some degree this can be avoided through a spatial aggregation of zones, but this intensifies measurement errors related to the estimates of spatial separation between workers and jobs. In general there is a more favorable trade-off between measurement errors and the number of commuters for more densely populated urban systems. In such a more compact system the commuting flow matrix potentially has not got very small entries, even if the zones are defined for relatively small areas, avoiding severe measurement errors.

The two matrices (27) and (28) are given from the procedure described in Section 4, on how estimated utilities are converted to efficient distances. (27) is based on $\hat{\beta}$ referring to distances measured in physical distance, while (28) reflects distances measured by traveling times. In evaluating the results notice first that some of the largest absolute deviations between measured and efficient distances are related to origin-destination combinations with few commuters. It follows from the commuting flow matrix (26) that our system has four entries with less than 2 commuters. As mentioned in Section 3, however, the system degenerates in situations with

zero-entries, and our estimation procedure is based on the assumption that there is one worker commuting from zone 3 to zone 13. According to our results the estimated efficient distances are considerably longer than measured distances for the origin-destination combinations with only one commuter. As a sensitivity experiment we re-estimated efficient distances in a case where the lowest entries are set equal to 2. This resulted in considerably smaller differences between measured and efficient distances corresponding to the relevant four combinations; the differences are reduced by an average of about 10, no matter which of the two measures of separation that is applied. It is reasonable that estimated revealed utilities corresponding to a particular option respond significantly to a doubling of observed commuting flows. The experimental increase in small entries has only marginal effects, however, on estimated efficient distances in the rest of the system.

This discussion indicates that caution must be exercised in interpreting the results, especially due to the presence of small entries in the commuting flow matrix, and to measurement errors related to the scaling and zoning of the geography. Still, there are some characteristic patterns in the estimated matrices of efficient distance that offer useful information about consumer preferences and traveling behavior in the region.

Notice first that the results are sensitive to the choice of separation measure in converting utilities to estimates of efficient distance. Speed limits and road categories are not homogeneous throughout the region, and the estimated pattern of efficient distances differs systematically as spatial separation is represented by physical distance or by traveling time. Consider for instance commuting flows from zone 13. With spatial separation measured by physical distance, the estimated efficient distances are shorter than the measured distances for all combinations involving more than 3 commuters. This corresponds to a tendency that the traveling speed at the relevant road links are higher than average in the transportation network, resulting in a situation with more commuting than expecting from the physical distance. This situation is more balanced in the case where spatial separation is measured by traveling time, reflecting that the measure distance is on average better corresponding to the perceived distance motivating commuting decisions.

As another example, consider commuting to and from zone 8, located at the edge of the most urbanized area in the region. In the case where spatial separation is measured by physical distance, the estimated efficient distances exceed measured distances for zones in the southern direction (zones 1-7). Once again the situation is considerably more balanced in the case where traveling time is assumed to be the relevant separation measure. This reflects the fact that

commuting between zone 8 and zones 1-7 involves intra-urban road links with lower speed limits than average in the regional transportation network. This is explicitly accounted for by the use of traveling time, and our estimation results indicate that the observed commuting flow between zone 8 and zones 1-7 correspond reasonably well to measured traveling times. To the degree that estimated efficient distances exceed measured distances also in this case, a possible explanation could be that commuting is deterred by the presence of congestion or other barriers in the road network. The estimation results for zone 8, however, offer no strong evidence that traveling time is an inadequate measure of spatial separation in explaining commuting flows. Congestion is no big problem in this geography.

For commuting between zone 8 and the rest of system the deviations between the estimated efficient and measured distances are not systematically dependent on the choice of separation measure. This indicates that the speed on the corresponding links is not deviating systematically from the average speed in the system.

We will not enter into a detailed further discussion of area-specific estimation results. Some characteristic patterns call for comments, however. Notice for instance that the estimated efficient distances exceed the measured distances for practically all commuting to and from zone 3. This applies for both measures of spatial separation. Zone 3 is separated from zones 4-13 by a bridge. As a relative estimate the deviations between efficient and measured distance are in particular large for commuting from the neighboring zones 4 and 5 on the mainland to zone 3. One reasonable explanation is that the bridge is perceived as a physical and/or mental transportation barrier. The bridge spans over a relatively long and windy distance, and is for instance in general inconvenient for biking and walking. To the degree that workers appreciate the opportunity to do their journeys-to-work by walking or biking, the origin-destination combinations involving the bridge are less attractive than other combinations, ceteris paribus. This effect primarily applies for short-distance commuting, and is an example of non-linearity in the determination of trip distribution.

For the other two zones on the Karmøy island (zones 1 and 2) our results reveal a clear tendency that traveling time is a preferred measure of spatial separation, capturing the fact that traveling speed is in general low on the relevant links.

Zones 9 and 10 are also examples where the estimated efficient distances systematically tend to exceed the measured distances, for both measures of spatial separation. In this case, however, there is no obvious explanation related to the transportation network. Due to the combinations

of favorable housing prices and a location of relative high accessibility in the local labor market, zones 9 and 10 has experienced a growing population for some years. This has resulted in a relatively high proportion of households with small children. For some individuals within this category the alternative of being offered a (part-time) job in the neighborhood might be to leave the labor force, for example due to practical problems of running a two-worker household. Zones 9 and 10 in general have a shortage of jobs, but a relatively high concentration of (local-sector) activities, depending on local demand.

A reasonable hypothesis, though without empirical evidence to be presented, is that local sector activities tend to employ workers who are spatially and professionally immobile. In such a situation a marked tendency might appear that local demand for labor is occupied with workers residing nearby, with a low reservation wage and a relatively high unwillingness to commute out of the neighborhood. This line of arguing offers one possible explanation why the observed commuting pattern results in high estimates of the efficient distances to and from zones 9 and 10.

Another argument related to the heterogeneity of jobs and workers can be used to explain the marked tendency of low estimated efficient distances for commuting to and from zone 11. This (relatively peripheral) zone has a dominating complex transporting and processing gas and condensate from the Norwegian continental shelf. This complex is demanding specialized labor that is recruited from the entire region. Observed commuting flows represent the net effect of distance deterrence considerations and wage/working considerations in a labor market equilibrium solution. The argument focusing on specialized jobs/workers also applies in an explanation of the low estimated efficient distances to and from zone 6, in the case where spatial separation is measured by traveling time. This zone hosts, for instance, the regional hospital and a University College in addition to a number of other activities typically located in a regional center.

6. An application to road pricing

Our approach can be used to study how a system with road pricing affects efficient distances and (dis)utilities. A toll ring is for instance being planned around the center (Haugesund) of the region used in the case study in Section 5. This toll ring is introduced primarily as a financing scheme for investments in road infrastructure, rather than for congestion management.

Based on observations of commuting flows before and after the introduction of road pricing we can in principle estimate the impact on efficient distances in terms of traveling time. Those estimates can be converted into monetary equivalents by using a reasonable estimate for the value of time. As a next step we can then find a system-wide, aggregated, estimate representing an important cost element related to the introduction of the toll ring. In a final evaluation of the financing scheme such costs can be compared to the benefits of improved road transportation network. Based on an ex post observation of traffic flows such benefits can in principle be estimated from the procedure that is described above.

As stated above caution must be exercised in interpreting the estimates of efficient distances based on an observation of a commuting flow pattern at a specific point in time. There are more reasons to trust estimates of changes in efficient distances over time. To the degree that measurement errors are constant in time the effects will be smoothed out in estimates of changes in efficient distances and utilities. This is analogous to the fact that differencing to eliminate time-constant effects might be a very effective method to obtain more reliable results in two-period panel data analysis, see for instance Wooldridge (2003).

The procedure suggested above has some weaknesses. One problem is that the response of increased traveling costs on commuting flows is typically slow. For an individual worker both the residential site and the employer are normally fixed for some time. Another dynamic aspect is that a toll ring in general initiates a dynamic process that might lead to changes in the marginal sums of a commuting flow matrix; both the residential location pattern and the spatial distribution of jobs might change as a results of the road pricing scheme. Those arguments mean that the measured response on commuting flows depends on the chosen time perspective. Ideally, our estimates of efficient distances and costs/benefits should refer to two states of spatial equilibrium. The process towards a new equilibrium solution is likely to be rather time-consuming, however. During the time required for a new equilibrium state to appear, the system most probably will be exposed for other exogenous shocks than those caused by the toll ring. Commuting flows are affected both by employment incidences in a business cycle and for instance by the development of new areas for residential purposes. Hence, in a long run time perspective the ceteris paribus interpretation applied in the evaluation of road pricing is not reasonable. All in all the interpretation of the results from the suggested approach is not straightforward in a case comparing commuting flows before and after the introduction of road pricing. Still, it might be useful and instructive to estimate revealed preferences in a system at such different points in time. It is also possible that the described approach is more appropriate for other trip purposes, like for instance shopping.

Road pricing policies can of course also be more deliberately designed for congestion management. As an example, Small et al. (2005) analyze a value-pricing experiment in the Los Angeles area. They consider a specific route where commuters can choose between express lanes at the cost of a toll, and regular freeway lanes, at the cost of reduced speed and reliability due to the presence of congestion. Small et al. (2005) study the choices between those two alternatives by combining revealed preference data and stated preference data from hypothetical situations that are aligned with the pricing experiment. The revealed preference data are based on a scenario where toll payments are charged through the use of an electronic transponder, allowing for hourly variation in toll rates. Based on a mixed logit model Small et al. (2005) estimate how commuters are deterred from the express lanes by higher toll rates and from the free lanes by longer and less reliable travel times. They also estimate how the implied values of time and reliability differ across individuals, by explicitly accounting for heterogeneity in preferences according to for instance income, age, and education. As stated in their concluding section such heterogeneity is necessary for value pricing to create significant benefits.

A scenario where the connection between two nodes in the transportation network are represented by alternative lanes can also be treated within the approach described in Section 5. Let each of the two zones/nodes appear twice in the commuting flow matrix. The link connecting one of the pairs is represented by the express lane, while the freeway lane is connecting the other pair. Based on an observation of a commuting flow matrix workers preferences for the two links can then be found through the estimation of efficient distances. Hence, we can obtain an estimate of how workers on average trade longer travel time and less reliability off against toll payments. By comparing with estimates of efficient distances in a situation with no toll, we can also estimate the aggregated net benefit of the pricing scheme. If data are available on the point in time when workers do their journeys-to-work, this procedure can for instance be made for each hour of a working day. It will then be possible to account for the impact of (time-dependent) variations in toll rates and of variations in expected travel times. This provides important information on how congestion pricing can be used to reach an efficient travel pattern. If data are available the estimates further can be made specific to categories of workers, accounting for heterogeneities with respect to for instance income, age, and education.

Small et al. (2005) focus on the effect of toll rates, travel times, and reliability (the predictability of travel time). Can our approach account for the effect of reliability? Assume that the system is in a state of user equilibrium, where the expected utility for an average commuter is the same for the two alternative routes. Since both toll rates and travel times are explicitly accounted for,

the difference between the estimated efficient distances for the express lane and the freeway lane can then be attributed to the effect of variations in reliability.

It is important to notice that it is possible to estimate the impact of road pricing also within an approach where the total regional commuting flow pattern is determined. It also was clear from the previous section that our approach in general contributes with important insight on how commuting flows are determined by characteristics of the region and the transportation network. We find, for instance, that traveling time should be used as a measure of spatial separation if speed limits and road categories are not homogeneous throughout the region. Our approach does not offer explicit parametric explanations of how alternative attributes influence commuting flows, but it represents a very useful input in a search for relevant variables in a more traditional spatial interaction model. The discussion in the previous section for instance introduces a hypothesis that labor market characteristics should be taken into account in an adequate explanation of commuting flows. Based on data from the same region such kinds of hypotheses are supported by Thorsen and Gitlesen (1998), within a competing destinations modeling framework.

7. Concluding remarks

In this paper we have outlined a new approach to the inverse gravity problem, i.e., to find a set of preferences $\mathbf{U} = \{U_{ij}\}_{i,j=1}^{N}$ such that the solution of the gravity model (1) replicates an observed tripdistribution $\mathbf{T} = \{T_{ij}\}_{i,j=1}^{N}$. In particular we have proved that there exist a unique set of preferences with zeros in the first line and the first column. To compute these preferences numerically, we have to solve a non-linear problem with a large number of parameters $(= (N - 1)^2)$. To overcome this problem we have proposed a new numerical algorithm that is able to handle problem with several hundred parameters.

If N is large, the solution is expressed in terms of a large number of parameters, and it can be very hard to extract explicit information from such a complex system. To facilitate interpretation, we have constructed a new theory that converts preferences to a uniquely defined set of efficient distances. To interpret the results we compare these efficient distances to the observed distances in the system. The basic idea is that when the efficient distance between two zones is longer(shorter) than the observed distance, then the flow between the nodes is smaller(larger) than aproiri expectations. Once this information is revealed, one can search for explanations for such kind of effects.

Our theory has been applied to a real world network using fairly up to date data (from 2004). The numerical findings shows that the notion of efficient distances is very well suited to reveal explicit

information about this particular system. To be more precise; when our model suggested that the efficient distance between two zones was considerably longer or shorter than the observed distance, then we could in most cases quickly come up with a logical explanation for that. Such explanations of course require that the analyst has detailed local knowledge about the network in question. When no such knowledge is available, we can still run and analyse a model of this kind, and there is good reason to believe that any profound effect found from such analysis corresponds to genuine effects in the system.

It is possible to run our model in quite singular cases, but special care must be taken if the observed matrix contains small entries. In such cases the model will often report spurious effects, and hence one should in normal cases not report results connected to such entries. To minimize problems of this sort one should seek to operate on a level of spatial aggregation were all entries are reasonably large.

In the paper we have also outlined a new line of approach to evaluate the impact of road pricing. The basic idea is then to convert efficient distances into monetary equivalents using a reasonable estimate for the value of time. If a pair of nodes are connected by several different links, we can use multiple listings of these nodes to indentify the traffic flow on each link. This again puts us in a position where we can compute efficient distances which in turn can be converted to monetary equivalents. While clearly an important issue, an empirical implementation of these ideas to a real world network is left for future research.

8. Appendix: Input and output data for the model in Section 5

The matrices (24),(25) and (26) below were used as input data to our model for the network in Section 5. In (26) we changed the entry $T_{3,13}$ from 0 to 1 to make the problem non-degenerate.

Based on the construction of efficient distances in Section 4, we computed efficient distance matrices for the network in Section 5. These computations were carried out as follows:

- Using the numerical algoritm in Section 3, we constructed a utility matrix U on the form (6) which provided perfect replication of the trip distribution (26) when we used the model in (1). The computation took several days, but computation time can probably be reduced considerably with a faster computer.
- We then computed 13 equivalent utility matrices $\mathbf{U}^{(1)}, \mathbf{U}^{(2)}, \dots, \mathbf{U}^{(13)}$, where each $\mathbf{U}^{(k)}$ was constructed as follows:

$$U_{ij}^{(k)} = U_{ij} - c_i - d_j$$

together with the 26 linear constraints

$$U_{ii}^{(k)} = 0, \ i = 1, \dots, 13$$
 $U_{ki}^{(k)} = U_{ik}^{(k)}, \ i \neq k$ $d_{13} = 0$

Hence for each k we have 26 contraints for the 26 constants $c_1, \ldots, c_{13}, d_1, \ldots, d_{13}$.

- Using (19), we put $\overline{U} = \frac{1}{13} \sum_{k=1}^{13} \mathbf{U}^{(k)}$.
- Using the distance matrix in (24) and the trip distribution in (26), we computed the best • replication (in the sense of loglikelihood) by a standard gravity model $\hat{\beta} = 0.0724434$, and used this in (20) to compute the efficient distance matrix (27).
- Using the distance matrix in (25) and the trip distribution in (26), we computed the best replication (in the sense of loglikelihood) by a standard gravity model $\hat{\beta} = 0.0651886$, and used this in (20) to compute the efficient distance matrix (27).

Γ 0	12.6	23.5	30.8	30.4	34.1	32.6	38.5	63.2	40.1	68.3	71.4	ך 93.5	
12.6	0	10.9	18.2	17.9	21.5	20.1	25.9	50.6	27.5	55.7	58.9	80.9	
23.5	10.9	0	7.3	7.	10.6	9.2	15.	39.7	16.6	44.8	48.	70.	
30.8	18.2	7.3	0	5.5	9.2	7.2	13.6	38.2	12.7	41.	44.1	66.1	
30.4	17.9	7.	5.5	0	3.7	3.8	8.	32.7	10.8	39.	42.1	76.5	
34.1	21.5	10.6	9.2	3.7	0	2.4	4.4	29.1	12.8	41.1	53.7	78.5	
32.6	20.1	9.2	7.2	3.8	2.4	0	5.2	29.9	10.6	38.8	41.9	64.	(24)
38.5	25.9	15.	13.6	8.	4.4	5.2	0	24.7	15.9	44.2	47.3	69.4	
63.2	50.6	39.7	38.2	32.7	29.1	29.9	24.7	0	28.3	49.2	40.8	65.7	
40.1	27.5	16.6	12.7	10.8	12.8	10.6	15.9	28.3	0	28.2	31.3	53.4	
68.3	55.7	44.8	41.	39.	41.1	38.8	44.2	49.2	28.2	0	47.5	68.5	
71.4	58.9	48.	44.1	42.1	53.7	41.9	47.3	40.8	31.3	47.5	0	27.6	
193.5	80.9	70.	66.1	76.5	78.5	64.	69.4	65.7	53.4	68.5	27.6	0]	

Distance matrix in km for the network in Section 5

Γ 0	15.3	29.3	40.	38.6	44.3	41.5	51.2	77.3	47.5	76.1	79.6	ך .111	
15.5	3 0	14.	24.7	23.3	29.1	26.2	35.9	62.	32.2	60.9	64.4	86.1	
29.3	3 14.	0	10.7	9.3	15.1	12.2	21.9	48.	18.2	46.8	50.4	72.1	
40.	24.7	10.7	0	8.2	14.	11.	20.9	47.	14.5	43.2	46.7	68.5	
38.0	6 23.3	9.3	8.2	0	5.8	6.3	14.6	40.7	11.6	40.3	43.7	65.5	
44.3	3 29.1	15.1	14.	5.8	0	4.5	6.8	33.	14.2	42.9	46.4	77.8	
41.5	5 26.2	12.2	11.	6.3	4.5	0	8.3	34.4	13.1	41.8	45.3	67.1	(25)
51.2	2 35.9	21.9	20.9	14.6	6.8	8.3	0	26.1	19.3	47.9	51.4	73.2	
77.3	3 <u>62</u> .	48.	47.	40.7	33.	34.4	26.1	0	26.8	47.6	47.8	63.6	
47.5	5 32.2	18.2	14.5	11.6	14.2	13.1	19.3	26.8	0	28.6	32.2	53.9	
76.1	1 60.9	46.8	43.2	40.3	42.9	41.8	47.9	47.6	28.6	0	47.1	64.6	
79.0	6 64.4	50.4	46.7	43.7	46.4	45.3	51.4	47.8	32.2	47.1	0	28.5	
L 111	. 86.1	72.1	68.5	65.5	77.8	67.1	73.2	63.6	53.9	64.6	28.5	0	

Traveling time (minutes) between the zones for the network in Section 5

Γ 1585	1211	180	62	142	436	26	33	2	14	11	11	8 J	
388	2060	315	107	243	590	49	46	8	24	39	11	10	
58	411	516	161	253	653	50	67	5	37	25	10	0	
36	253	155	365	386	1002	109	104	3	110	70	21	4	
23	180	71	116	425	1064	122	92	9	72	62	27	4	
30	187	109	114	322	1582	190	163	17	86	70	42	4	
15	133	65	76	276	1092	248	143	15	66	46	25	4	(26)
28	163	100	119	454	1875	278	443	36	92	80	22	8	
14	45	29	29	119	452	51	77	573	48	23	25	4	
10	97	67	59	288	600	91	62	13	809	165	68	19	
5	25	10	9	79	167	20	18	8	266	422	27	10	
5	27	10	12	86	185	18	12	1	82	33	1324	297	
4	13	1	3	18	93	3	4	1	24	9	405	1307	

Commuting flow matrix in Section 5

Γ 0	13.8	26.8	36.5	35.5	35.1	47.4	44.6	77.7	64.1	67.3	72.9	ך 75.2	
13.	0	12.6	22.5	21.7	24.5	32.2	33.5	52.2	50.2	43.4	66.5	65.7	
33.4	16.4	0	11.	15.3	17.2	26.1	22.5	52.8	38.4	43.7	62.	91.6	
40.2	23.4	16.9	0	9.7	11.6	15.6	16.7	60.2	23.7	29.8	52.	72.8	
38.	19.7	19.2	7.4	0	2.4	5.6	10.	36.6	21.1	23.	40.2	64.4	
37.5	22.3	16.4	10.8	6.9	0	2.6	5.2	30.9	21.8	24.5	37.2	67.5	
48.1	28.	24.6	17.4	10.1	6.2	0	8.1	33.7	26.5	31.3	45.4	68.5	(27)
47.	32.7	26.2	18.7	10.8	6.2	5.9	0	29.1	29.4	31.2	54.7	66.5	
65.6	59.6	52.3	47.3	38.3	34.9	38.4	33.2	0	47.5	57.5	62.	85.1	
61.7	40.5	32.3	29.	17.7	22.6	22.	27.8	43.8	0	21.8	39.7	55.1	
62.4	50.4	49.7	46.2	26.7	31.4	34.1	36.	41.7	6.5	0	43.6	55.2	
72.5	59.5	59.9	52.3	35.6	40.1	45.6	51.7	80.5	32.9	45.3	0	18.5	
L77.7	71.5	93.6	73.4	59.2	51.6	72.3	68.9	82.5	51.8	65.2	18.3	0]	

Efficient distances in km

$ \begin{bmatrix} 0 \\ 14.4 \\ 37.1 \\ 44.7 \\ 42.3 \end{bmatrix} $	$15.3 \\ 0 \\ 18.3 \\ 26. \\ 21.9$	$29.8 \\ 14. \\ 0 \\ 18.8 \\ 21.4$	$\begin{array}{c} 40.5 \\ 25. \\ 12.3 \\ 0 \\ 8.2 \end{array}$	$39.5 \\ 24.1 \\ 17. \\ 10.8 \\ 0$	$39. \\ 27.2 \\ 19.2 \\ 12.9 \\ 2.6$	52.7 35.8 29. 17.3 6.3	$\begin{array}{c} 49.6 \\ 37.3 \\ 25.1 \\ 18.6 \\ 11.1 \end{array}$	$86.4 \\ 58. \\ 58.8 \\ 66.9 \\ 40.7$	$71.3 \\ 55.8 \\ 42.7 \\ 26.3 \\ 23.5$	$74.8 \\ 48.2 \\ 48.6 \\ 33.1 \\ 25.6$	$81.1 \\73.9 \\68.9 \\57.8 \\44.6$	$83.6 \\ 73. \\ 101.9 \\ 80.9 \\ 71.6$	
$\begin{array}{c} 42.3 \\ 41.6 \\ 53.4 \\ 52.2 \\ 72.9 \\ 68.5 \end{array}$	$21.9 \\ 24.8 \\ 31.2 \\ 36.4 \\ 66.2 \\ 45.$	$ \begin{array}{r} 21.4 \\ 18.3 \\ 27.4 \\ 29.1 \\ 58.2 \\ 35.9 \\ \end{array} $	$ \begin{array}{c} 8.2 \\ 12. \\ 19.4 \\ 20.8 \\ 52.6 \\ 32.3 \\ \end{array} $	$ \begin{array}{c} 0\\ 7.7\\ 11.3\\ 12.\\ 42.6\\ 19.6 \end{array} $	$ \begin{array}{c} 2.0 \\ 0 \\ 6.8 \\ 6.9 \\ 38.8 \\ 25.1 \end{array} $	$ \begin{array}{r} 0.3 \\ 2.9 \\ 0 \\ 6.6 \\ 42.7 \\ 24.4 \end{array} $	$ \begin{array}{r} 11.1 \\ 5.8 \\ 9. \\ 0 \\ 36.9 \\ 30.9 \\ \end{array} $	$ \begin{array}{r} 40.7 \\ 34.4 \\ 37.5 \\ 32.4 \\ 0 \\ 48.7 \end{array} $	$23.3 \\ 24.2 \\ 29.4 \\ 32.7 \\ 52.8 \\ 0$	$23.0 \\ 27.2 \\ 34.8 \\ 34.7 \\ 63.9 \\ 24.2$	$ \begin{array}{r} 44.0\\ 41.3\\ 50.4\\ 60.8\\ 68.9\\ 44.1 \end{array} $	$71.0 \\ 75. \\ 76.2 \\ 73.9 \\ 94.6 \\ 61.3$	(28)
69.4 80.6 86.4	56. 66.1 79.5	$55.3 \\ 66.6 \\ 104.1$	52.5 51.3 58.2 81.6	$ \begin{array}{r} 19.0 \\ 29.7 \\ 39.6 \\ 65.8 \end{array} $	$ \begin{array}{r} 23.1 \\ 34.9 \\ 44.6 \\ 57.3 \end{array} $	$ \begin{array}{r} 24.4 \\ 37.9 \\ 50.7 \\ 80.4 \end{array} $	$ \begin{array}{r} 50.9 \\ 40. \\ 57.5 \\ 76.6 \end{array} $	46.3 89.5 91.7	$7.3 \\ 36.6 \\ 57.6$	$ \begin{array}{c} 24.2 \\ 0 \\ 50.4 \\ 72.5 \end{array} $	$ \begin{array}{r} 44.1 \\ 48.5 \\ 0 \\ 20.4 \end{array} $		

Efficient distances in minutes

REFERENCES

Anas, A. 1983. Discrete choice theory, information theory and the multinomial logit and gravity models. *Transportation Research B* 17, 13–23.

Barkely, D. L., Henry M. S., Bao S., Brooks K. R. 1995. How functional are economic areas? Tests for intra-regional spatial association using spatial data analysis, *Papers in Regional Science* 74, 297–316.

Bregman, L. M. 1967. The relaxation method of finding the common point of convex sets and its application to the solution of problems in convex programming. USSR Computational Mathematics and Mathematical Physics 7, 200–217.

Erlander, S., Smith. T.E. 1990. General representation theorems for efficient population behavior. *Applied Mathematics and Computation 36*, 173–217.

Erlander, S., Stewart. N. F. 1990. The gravity model in transportation analysis - theory and extensions, VSP: Utrecht.

Jörnsten, K., Ubøe J. *Efficient Statistical Equilibria in Markets*. Discussion paper 2005/2, Norwegian School of Economics.

Sen, A., Smith T. E. 1995. *Gravity Models of Spatial Interaction Behavior*. Springer-Verlag: Berlin.

Small, K. A., Winston, C., and Yan, J. 2005. Uncovering the distribution of motorists preferences for travel time and reliability, *Econometrica* 73, 1367–1382.

Thorsen, I., and Gitlesen, J-P. 1998. Empirical Evaluation of Alternative Model Specifications to Predict Commuting Flows, *Journal of Regional Science* 38 (2), 273–292.

Wilson, A. G. 1967. A statistical theory of spatial distribution models. *Transportation Research* 1, 253–269.

Wooldridge, G. M. 2003. Introductory Econometrics: A Modern Apprach, Thomson, South-Western.